MEASUREMENT OF ENERGETIC EFFICIENCY OF ELECTRON EMISSION UNDER LOW ENERGY ELECTRON BEAM IRRADIATION: APPLICATION TO HALL THRUSTER DIELECTRIC WALLS

Marc Villemant[(1)], Pierre Sarrailh[(1)], Mohamed Belhaj[(1)], Laurent Garrigues[(2)], Claude Boniface[(3)]

[(1)]ONERA, The French Aerospace Lab, Département Environnement Spatial- DESP, Toulouse, France, Email:marc.villemant@onera.fr
[(2)] Laboratoire Laplace, Laboratoire plasma et conversion d'énergie, Toulouse, France, Email:laurent.garrigues@laplace.univ-tlse.fr
[(3)] CNES, Service Propulsion Pyrotechnie et Aérothermodynamique, Toulouse, France, Email:claude.boniface@cnes.fr

ABSTRACT

From its discovery until nowadays, electrons emission (EE) has been thoroughly studied and has allowed numerous technologies development. Among them, RADAR, Scanning Electron Microscope and scintillators can be quoted. EE can also be a parasitic phenomenon especially for space applications (multipactor effect in wave guides, spacecraft charging, etc.). Until now, EE has essentially been described for high incident energy (superior to 100 eV). However several technologies are being developed which involved EE with low incident energy (below 100 eV). One of them is plasma thrusters for satellites applications. Toward this work, low energy EE impact (below 100 eV) on energetic balance in Stationary Plasma Thrusters (SPTs) will be discussed as well as method of measurement of this impact.

1. INTRODUCTION

Electronic Emission (more precisely electrons impact induced electronic emission) is the emission of electrons from a material submitted to an incident electrons flow (as described in *Figure 1*).

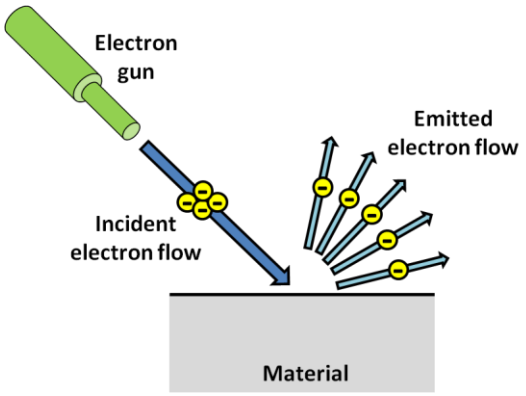

Figure 1 Experimental principle of electronic emission

It is a phenomenon with a non-negligible impact on numerous technology of space industry. For example, it is shown throughout simulation that EE can have a significant impact on SPTs operation [1], [2].

1.1. Description of EE

Several questions are emerging about EE: How many electrons are emitted, with which energy/speed, to which direction? In order to answer these three questions three elements are observed: the Total Electron Emission Yield (TEEY, cf. *Figure 2*), the energy distribution function (cf. *Figure 3*), and the angular distribution of emitted electrons (cf. *Figure 9* and *Figure 10*).TEEY depends on incident electrons energy and is defined as:

$$\sigma(E_0) = \frac{N_s}{N_0} \qquad (1)$$

Where, N_s is the number of emitted electrons and N_0 is the number of incident electrons

The emitted electrons can be divided in three categories: the reflected electrons, the secondary electrons and the backscattered electrons.

Reflected electrons are not penetrating the surface and are directly reemitted in the vacuum. They represent a negligible part of the EE. Their contribution to TEEY is represented by the reflection coefficient R.

Secondary electrons are mostly electrons from the material (valence band, defects bands or conduction band) which are extracted from it by receiving a sufficient amount of kinetic energy from an incident electron. Some of them diffuse eventually to the surface and are emitted. Their energy is relatively low and, except for very low incident electrons energy ($< 20\ eV$), they represent the majority of EE (cf.*Figure 3*). Their contribution to TEEY is represented by the Secondary Electronic Emission Yield (SEEY):δ.

Finally backscattered electrons, which represent the second most important fraction of EE, except for $E_0 < 20\ eV$, are divided into two categories: elastically and non-elastically backscattered electrons. Elastically backscattered electrons are enduring elastic collisions only. Thus they are not enduring energy losses in the material. Consequently, they are emerging from the

material with energy equal to incident energy (cf. High energy peak on *Figure 3*). Non-elastically backscattered electrons have transferred a part of the energy to the material due to inelastic collisions but still have enough energy to overcome the vacuum/material barrier. They are represented by the blue dashed line on *Figure 3*, minus the elastic peak. Backscattered electrons contribution to TEEY is represented by backscattering coefficient η. In the end, we have:

$$\sigma = R + \delta + \eta \approx \delta + \eta \qquad (2)$$

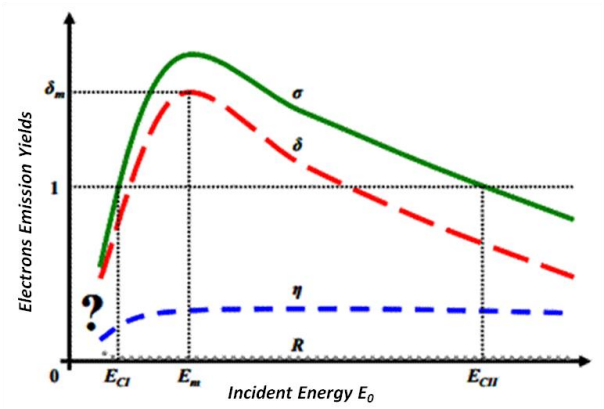

Figure 2 TEEY representation as a function of incident electron s energy for high Z material with contribution of different electrons types [3]

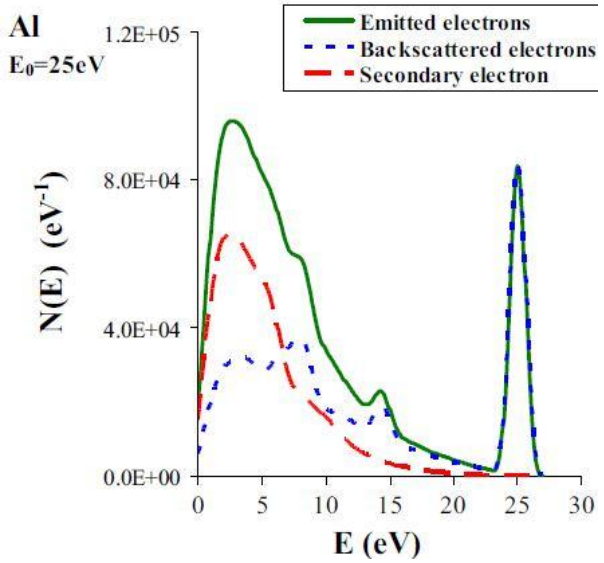

Figure 3 Calculated energy distribution of emitted electrons for Aluminium irradiated with electrons at 25eV [3]

1.2. Electron Emission Models

In the scientific literature, numerous models can be found which describe EE. Nonetheless they generally limit themselves to Total Electron Emission Yield (TEEY) or even at Secondary Electrons Emission Yield (SEEY). Only a few give the energetic distribution of emitted electrons and only of secondary electrons [4]. These models are based on the transfer of energy from incident electron to the material (Widdington's law [5], power law [6], constant loss model [6], irradiated volume model [7]). Thus it appears that energy balance at the wall is important to understand low energy EE phenomena.

1.3. Listing of phenomena taking part in EE

On the energy balance point of view, it could appear evident that not all the energy of the incident electron is transferred to the emitted electrons. Macroscopically, several phenomena depend on energy transfers from incident electrons to the material. If they interact strongly with atomic bonding, they can create erosion and material ageing. Besides if they interact with the free electron gas or electron net, they can create a plasmon displacement and thus improve the conductivity of the material, in that case it is question of Radiation Induced Conductivity (RIC) [8]. They can also transfer energy to phonons (especially in dielectrics) and thus generate heat. They can finally transfer enough energy to an intern electron to make him become a secondary electron. It creates in that case Secondary Electron Emission (SEE).

Considering plasma/wall interactions, it can be seen that it is not sufficient to consider independently the number of incident and emitted electrons on one hand and their energetic distributions on the other hand, because none of them represent the energy balance at the wall. A new value combining TEEY and energy distribution could allow giving an idea of energetic properties of a plasma/wall energy exchange.

2. DEFINITION OF ENERGETIC EFFICIENCY

The energetic efficiency of plasma/wall interaction, noted η_E is defined as the kinetic energy of electrons emitted to plasma, divided by the kinetic energy of the electrons incident to the wall (cf. *Figure 4*). It will then be defined analytically by:

$$\eta_E = \frac{E_s}{E_0} = \frac{E_0 - E_{abs}}{E_0} = 1 - \frac{E_{abs}}{E_0} \qquad (3)$$

Where, E_s is the kinetic energy of electrons emitted from the wall [eV], E_0 is the kinetic energy of electrons incident to the wall [eV] and E_{abs} is the energy diffused by incident electrons in the wall [eV]

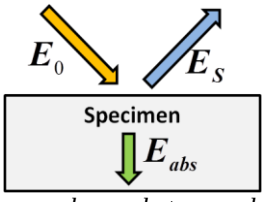

Figure 4 Energy exchange between plasma and wall

In many cases of non-equilibrium plasmas, the overwhelming part of plasma/wall interaction is due to electrons/wall interaction. If we approximate η_E by electrons contribution only, it can be written that:

$$\eta_E = \frac{N_s \int_0^{+\infty} E.f_s(E).dE}{N_0 \int_0^{+\infty} E.f_0(E).dE} = \sigma(E_0)\frac{\int_0^{+\infty} E.f_s(E).dE}{\int_0^{+\infty} E.f_0(E).dE} \quad (4)$$

Where, $N_s$is the number of emitted electrons, N_0 is the number of incident electrons $[\emptyset]$, f_s is the distribution function of emitted electrons $[eV^{-1}]$, f_0 is the distribution function of incident electrons $[eV^{-1}]$ and $\sigma(E_0)$is the Total Electrons Emission Yield (TEEY).
The objective of this work is to give experimental values of η_E for miscellaneous materials and of their evolution with incident electrons energy.

3. EXPERIMENTAL PROTOCOL

We will now describe the experimental protocol which allowed deducing first values of energetic efficiency of plasma/wall interaction.

3.1. Experimental protocol principle

A monoenergetic incident electrons beam was generated by an electron gun at the energy E_0. TEEY and emitted electrons energy spectres were measured for various E_0between 5 eV and 105 eV.
As the incident electron flow is quasi-monocinetic (energy spread 0.6 eV [9]), η_E expression can be simplified to:

$$\eta_E = \sigma(E_0) \cdot \frac{\int_0^{+\infty} E.f_s(E).dE}{E_0} = \sigma(E_0) \cdot \frac{[E_s]}{E_0} \quad (5)$$

Where, $[E_s]$ is the mean energy of emitted electrons $[eV]$ and it has been supposed that distribution functions are normalized, i.e:

$$\int_0^{+\infty} f(x).dx = 1 \quad (6)$$

However, experimentally, we have to approximate this integrated value of emitted electrons mean energy. Thus:

$$\eta_E \approx \frac{\sigma(E_0)}{E_0} \cdot [E_s]_N \quad (7)$$

With $[E_s]_N$ the numerical mean value in eV.

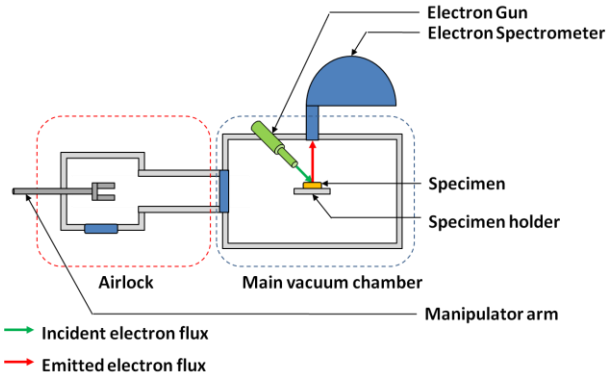

Figure 5 DEESSE test-bed scheme (DESP,ONERA)

Test-bed descriptionExperiments have been performed on DEESSE (DESP, ONERA) [10]. The measurement principle is to irradiate a specimen of a given material and to measure both the emitted electrons spectre and TEEY [9]. It is important to notice that all the data are given for the emitted energy flux through the control surface of the analyser time the amplification factor of the analyzer.
Silver, graphite and a thin layer of SiO_2 have been successively analysed. Then, by using *(7)* we can deduce experimentally the energetic efficiency.

3.2. Extrapolation to Maxwellian distributed plasma

In order to give data that could be used in space field, we average these values on a Lambertian distribution. That is, the distribution of an electrons gas in thermal equilibrium which is observed through a surface.

$$[\eta_E]_{\mathcal{L}}(T) = \frac{\int_0^{+\infty} \eta(E_0) f_{\mathcal{L}}(E_0,T).dE_0}{\int_0^{+\infty} f_{\mathcal{L}}(E_0,T).dE_0} \quad (8)$$

As this distribution is normalized, it can be written that:

$$[\eta_E]_{\mathcal{L}}(T) = \int_0^{+\infty} \eta(E_0) f_{\mathcal{L}}(E_0,T).dE_0 \quad (9)$$

These results are superimposed to monoenergetic ones on *Figure 6*, *Figure 7*, *Figure 8* and *Figure 11*.

4. EXPERIMENTAL RESULTS

Experimental results have been obtained for three different materials: technical silver (i.e. silver exposed to ambient atmosphere), graphite, and SiO_2.

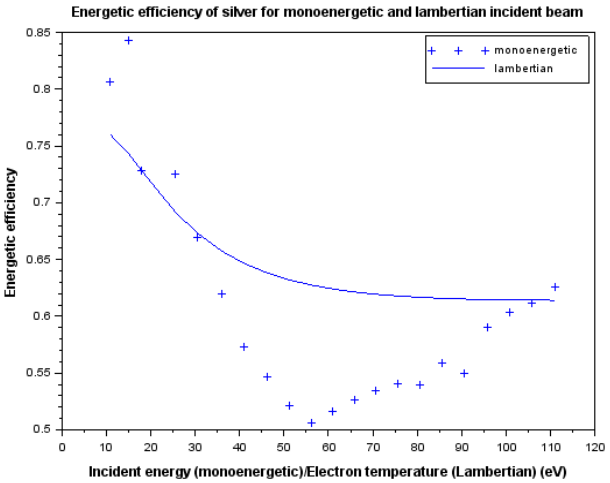

Figure 6 Silver energetic efficiency of plasma/wall interaction

Figure 6 represents the energetic efficiency of silver specimen under electron incident beam at normal incidence. η_E values have been read every 5 eV for E_0 values between 10 eV and 110 eV.
It can be observed that η_E is high at low energy (around 80%) and decrease until reaching a minimum value of 51% at 55 eV. It increases again a bit slower until 110 eV, where it reaches 64%. As for as the Lambertian distribution values are concerned, it can be observed a smoother, monotonic shape which decrease from 77% to 63% between 5 and 110 eV.

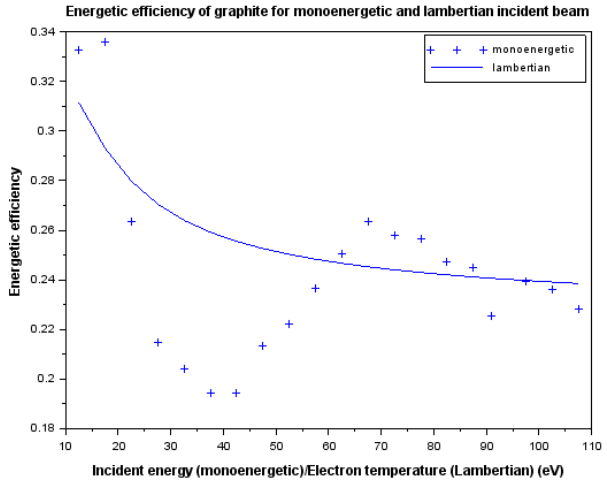

Figure 7 Graphite energetic efficiency of plasma/wall interaction

Figure 7 represents the energetic efficiency of graphite specimen under electron incident beam at normal incidence. η_E values have been read every 5 eV between 10 eV and 110 eV. The same global shape as for silver can be observed on *Figure 7*. However η_E values are much lower here (between 19% and 34%).

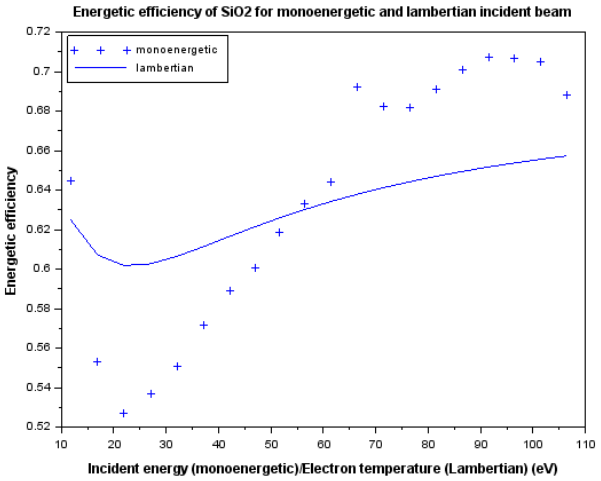

Figure 8 SiO2 energetic efficiency of plasma/wall interaction

Figure 8 represents the energetic efficiency of SiO_2 thin layer (10 nm) specimen under electron incident beam at normal incidence. η_E values have been read for E_0 going from 10 eV and 110 eV and set every 5 eV between.
A more complicated shape can be observed here. A first stiff decrease from 65% to 53% can be observed between 10eV and 25 eV followed by an increase from 53% to 70% on the range 25 to 90 eV. However, unlike graphite and silver, the curve reaches a maximum here before decreasing again. However due to the range of values we are using, it is difficult to give an estimation of the curve shape above 90 eV. If the Lambertian data are now considered, a non monotonic shape is still observed, which decrease from 63% to 60% between 5 eV and 20 eV. Then, an increase is observed: from 60% to 65% on the 20-110 eV range.

These measurements show a non negligible variation of energetic efficiency from one material to another and also a dependency in electron temperature of energetic efficiency. None of these two observations has been taken into account in the current models of EE applied to SPTs.
Nonetheless, if these experiments give quantitative results, one should recognize that they are not simple to realize and that numerous uncertainty should be considered and balanced. Provided that, the results will be quantitatively accurate.

5. MEASUREMENT ACCURACY

Detected uncertainties will be analyzed and the way they are taken into account will be exposed thereafter.

5.1. Surface charging

One of the recurring problems is that dielectric materials will get a surface charge which will vary with incident electrons [11]. However this bias can be easily corrected and the surface potential can be deduced from it. As a

matter of fact, on the energy spectres, an energy offset can be observed with no electron emission for emitted electron energy close to zero. And we know from Chung and Everheart model [4] that secondary electrons are emitted from 0 eV to $+\infty$.

5.2. Emitted electrons anisotropy

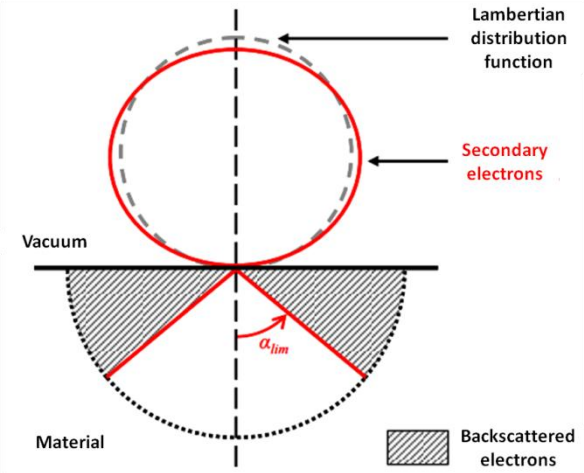

Figure 9 Scheme of angular distribution of secondary electrons [3]

One of the other points which has to be handled is the anisotropy of emitted electrons. It can be observed, on *Figure 9*, that the angular distribution of the secondary electrons is almost Lambertian [3] for polycrystalline and amorphous materials . However the backscattered electrons are, on the contrary very anisotropic as it can be seen on *Figure 10* [3].

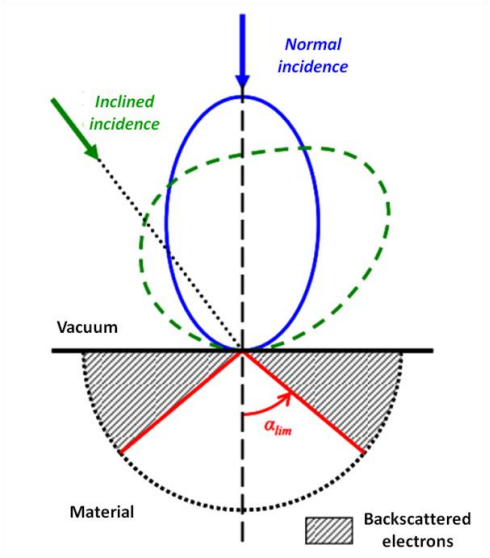

Figure 10 Scheme of backscattered electrons angular distribution [3]

Thus, as a function of the analyzer position, the recorded spectre may differ as function of the acceptance angle. This may probably induce an important uncertainty on measurements.

5.3. Distribution function deformation with surface charge

One of the other points that can have a non negligible effect on measurements accuracy is the deformation of electrons distribution due to their transport between the surface and the analyzer. It has been observed on silver specimen that, depending on the sample voltage bias η_E values will vary significantly (cf. *Figure 11*).
Indeed, we can see, on *Figure 11*, η_E evolution in function of incident energy for three different surface potential. Both values for monoenergetic and Lambertian distributed incident electron beam have been plotted.
We can recognize on *Figure 11* the typical form of monoenergetic and Lambertian distribution function curves that we have already seen in *Figure 6* to *Figure 8*. It can be observed, also, that monoenergetic curves are not monotonic. They start from a high value (between 63% and 80%) at 5eV, decrease until reaching a value between 45% and 47% around 60 eV before very slightly increasing to a value between 46% and 49%. Depending on the surface potential a deviation can be observed between the different curves. For a high surface potential (15V) η_E values are, averagely, more important than for a 10V or 5V surface potential. Between 25 and 35 eV, a gap of 12% can be observed between 15V and 10V and of 7% between 10V and 5V. These deviations become negligible at high energy (approximately 3% around 100 eV).

These experimental values show that, even if the global shape of the curve is accurate, there are some improvements to perform on the experimental protocol and data processing before getting very accurate quantitative results.

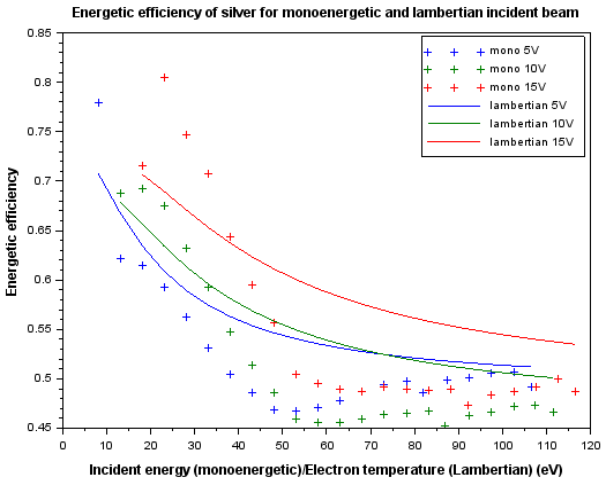

Figure 11 Experimental results of energetic efficiency for various imposed surface potential

One explanation which seems plausible is that surface potential modified the angular distribution of emitted electrons by replying the SE, leading to the distortion the emission lobs normally to the surface.

6. ANALYSIS

It can be interesting now to inspect the implications that these measurements could have as for as SPTs application is concerned.

6.1. Electron/wall predominance in plasma/wall energy balance

Electrons can have a predominant role in energetic balance of plasma thrusters. In order to observe it, an energy balance to the wall can be considered. First of all, it can be observed that in steady state, the charge balance at the wall (cf. **Erreur ! Source du renvoi introuvable.**) is equal to zero, that is:

$$J_{e0} + J_{ee} + J_i = 0 \qquad (10)$$

Where, J_{e0} is the thermal electron flux from plasma, $J_{ee} = -\sigma \cdot J_{e0}$ is the flux of emitted electrons and J_{i0} is the ion flux from the plasma
Thus, there is:

$$J_i = -J_{e0}(1-\sigma) \qquad (11)$$

It can be observed thus, that for $\sigma \sim 1$, the current of thermal electrons collected from the plasma is well higher than the current of ions.
In term of energy, by supposing that the electrons temperature is equal to ion energy, this equation transforms into:

$$\frac{P_i}{P_e} = \frac{1-\sigma}{1-\eta_E} \qquad (12)$$

It can be observed thus, that for $\sigma \sim 1$, the energy balance is dominated by the electrons $\frac{P_i}{P_e} \approx 0$. Thus, the energy efficiency yield could be a key parameter in the energy balance computation.

6.2. Consequences of η_E measurement on SPT modelling

In the measurements done, a non-negligible variation of η_E is observed, it could suggest that an improvement of the current models is possible. As a matter of fact, if we consider calculations realised on SPTs performances by Katz and Goebl [12], a constant loss at the wall is generally considered. It could be interesting to rewrite these calculations taking these experimental data into account.
Moreover current Particle In Cell models (plasma particles models based on Monte-Carlo method) are today 1D or 2D [1], [2], [13] (a 3D model is impracticable today due to computation cost of such a simulation). In order to take EE into account, they use an energy balance to reinsert in the plasma electrons with a total energy depending on the chosen loss model at the wall. Until now, loss model at the wall has been assumed constant or linear. It could be interesting to use these experimental data in order to see if it could impact the global modelling.

7. CONCLUSION AND FURTHER STUDIES

This work shows which problems arise when it is tried to measure accurately the energetic efficiency of plasma/wall interaction, and by extension, how difficult it is to measure a relevant energy spectre for a material. However, even if experimental data will need more investigation to give accurate quantitative results, they show yet an important variation along the 0-100 eV incident energy range. This could have a non-negligible impact on SPTs modelling and miscellaneous other applications.
In order to take into account the uncertainty linked to angular distribution of EE, one of the ONERA test-beds (CELESTE test-bed, DESP, ONERA) has been modified in order to control the angular position of the analyzer and thus to be able to integrate measurements on a π-angle. It is hoped that this would solve the bias due to angular anisotropy and surface potential influence on angular distribution.

8. ACKNOWLDGEMENTS

This PhD works has received an ONERA/CNES funding. Moreover, the authors wish to thank Dr. Makasheva for preparing SiO_2 thin layer specimens.

9. REFERRENCES

[1] D. Sydorenko, A. Smolyakov, I. Kaganovich, and Y. Raitses, 'Kinetic simulation of secondary electron emission effects in Hall thrusters', *Phys. Plasmas*, vol. 13, no. 1, p. 014501, 2006.

[2] A. Héron and J. C. Adam, 'Anomalous conductivity in Hall thrusters: Effects of the non-linear coupling of the electron-cyclotron drift instability with secondary electron emission of the walls', *Phys. Plasmas 1994-Present*, vol. 20, no. 8, p. 082313, Aug. 2013.

[3] J. Roupie, 'Contribution à l'étude de l'émission électronique sous impact d'électrons de basse énergie (<= 1keV): application à l'aluminium', Toulouse, ISAE, 2013.

[4] M. S. Chung and T. E. Everhart, 'Simple calculation of energy distribution of low- energy secondary electrons emitted from metals under electron bombardment', *J. Appl. Phys.*, vol. 45, no. 2, pp. 707–709, Feb. 1974.

[5] E. M. Baroody, 'A Theory of Secondary Electron Emission from Metals', *Phys. Rev.*, vol. 78, no. 6, pp. 780–787, Jun. 1950.

[6] R. G. Lye and A. J. Dekker, 'Theory of secondary emission', *Phys. Rev.*, vol. 107, no. 4, p. 977, 1957.

[7] J. Cazaux, 'A new model of dependence of secondary electron emission yield on primary electron energy for application to polymers', *J. Phys. Appl. Phys.*, vol. 38, no. 14, p. 2433, 2005.

[8] T. P. Rachel Hanna, 'Radiation induced conductivity in space dielectric materials', *J. Appl. Phys.*, vol. 115, no. 3, 2014.

[9] GINESTE T., *Emission électronique sous impact d'électrons : applications spatiales. Thèse soutenue le 19 Novembre 2015 pour l'obtention du diplôme de Doctorat de l'Université de Toulouse délivré par l'ISAE.* 2015.

[10] D. P. N. Balcon, 'Secondary Electron Emission on Space Materials: Evaluation of the Total Secondary Electron Yield From Surface Potential Measurements', *Plasma Sci. IEEE Trans. On*, vol. 40, no. 2, pp. 282 – 290, 2012.

[11] J. Cazaux, 'Some considerations on the secondary electron emission, δ, from e− irradiated insulators', *J. Appl. Phys.*, vol. 85, no. 2, pp. 1137–1147, Jan. 1999.

[12] D. M. Goebel and I. Katz, *Fundamentals of Electric Propulsion*. Hoboken, New Jersey: John Wiley&Sons, INC., 2008.

[13] P. Coche and L. Garrigues, 'A two-dimensional (azimuthal-axial) particle-in-cell model of a Hall thruster', *Phys. Plasmas*, vol. 21, no. 2, p. 023503, Feb. 2014.